

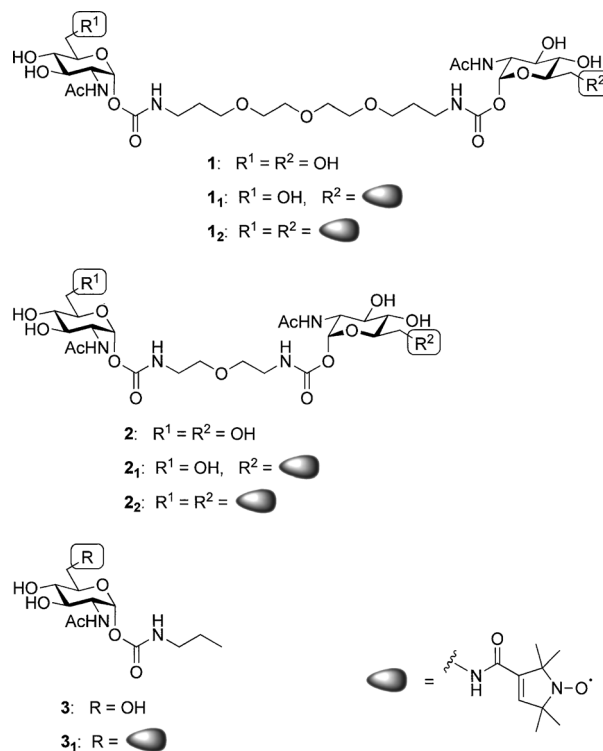
Mechanism of Multivalent Carbohydrate–Protein Interactions Studied by EPR Spectroscopy**

Patrick Braun, Bettina Nägele, Valentin Wittmann,* and Malte Drescher

Dedicated to Professor Richard R. Schmidt

The interaction of multivalent carbohydrate derivatives with carbohydrate-binding proteins (lectins) is frequently observed in biological systems, and their inhibition by tailored multivalent ligands is a powerful strategy for the treatment of many human diseases.^[1] Compared to monovalent interactions, multivalency can lead to significantly increased binding affinities and specificities. Several mechanisms have been suggested to be responsible for the observed binding enhancements.^[1,2] Among them is the spanning of adjacent binding sites by the multivalent ligand (chelate effect)^[3] to which the highest contribution to enhanced binding affinity is attributed. Recently, we were able to characterize chelating binding of multivalent *N*-acetylglucosamine (GlcNAc) derivatives to wheat germ agglutinin (WGA) by X-ray crystallography.^[4] Since it is well established that the structure of biomolecules determined by X-ray crystallography is not necessarily identical to their solution structure^[5] and, furthermore, binding mechanisms in a densely packed crystal and in solution may differ, a method to determine the binding mode of multivalent interactions in solution is desirable. Here, we describe the application of electron paramagnetic resonance (EPR) spectroscopy of spin-labeled ligands for this purpose and provide structural evidence for chelating binding of a multivalent GlcNAc derivative to WGA in solution.

WGA is a plant lectin that forms a 36 kDa stable homodimer with a twofold symmetry axis and is specific for terminal *N*-acetylneuraminic acid and GlcNAc.^[6] WGA contains eight binding sites, termed A1, B1C2, C1B2, D1A2, A2, B2C1, C2B1, and D2A1.^[7] We could show by X-ray crystallography that four molecules of divalent ligand **1** (Scheme 1) simultaneously bind to all eight GlcNAc binding sites of the WGA dimer with each ligand bridging pairs of adjacent binding sites, specifically, B1C2–C2B1, B2C1–C1B2, A1–D2A1, and A2–D1A2.^[4] This structure explains the high binding affinity of **1** towards WGA ($IC_{50} = 57 \mu M$)^[4] that had



Scheme 1. Mono- and divalent WGA ligands.

been determined by an enzyme-linked lectin assay (ELLA).^[8] Divalent ligand **2** with a shorter linker has an IC_{50} value of $734 \mu M$, and monovalent GlcNAc derivative **3** has an IC_{50} value of $8 mM$.^[4]

Employing a combination of continuous-wave (cw) EPR spectroscopy and a two-frequency pulsed EPR method utilizing analogues of **1**, **2**, and **3** containing either one (**1**₁, **2**₁, **3**₁) or two (**1**₂, **2**₂) nitroxide spin labels (Scheme 1), we now present evidence for the chelating binding of **1** in frozen glassy solution. In contrast, ligand **2** with the shorter linker between the GlcNAc residues is shown to not be able to bridge adjacent binding sites of the lectin but to rather bind monovalently.

The double electron–electron resonance (DEER or PELDOR)^[9] technique can be used to measure distributions of long distances between spin labels separated by up to 10 nm and is, therefore, ideally suited for the study of multivalent ligand–protein interactions. To the best of our knowledge, this powerful technique here is used for the first time in this context. Distances less than 1.5 nm are not

[*] Dipl.-Chem. P. Braun, M. Sc. B. Nägele, Prof. Dr. V. Wittmann, Dr. M. Drescher

University of Konstanz, Department of Chemistry
 and Konstanz Research School Chemical Biology (KoRS-CB)
 78457 Konstanz (Germany)
 Fax: (+49) 7531-88-4573
 E-mail: mail@valentin-wittmann.de

[**] This work was supported by the Deutsche Forschungsgemeinschaft (DR 743/2-1), the University of Konstanz, and the Konstanz Research School Chemical Biology. We thank Martin Spitzbarth, Tim ten Brink, and Dr. Thomas Exner for contributions to data analysis.

Supporting information for this article is available on the WWW under <http://dx.doi.org/10.1002/anie.201101074>.

accessible by DEER^[10] but were detected by low-temperature cw EPR. Rotational mobility was determined by cw EPR at ambient temperature using singly labeled ligands. Examination of the crystal structure of the complex of **1** and WGA (PDB ID: 2X52)^[4] revealed that the hydroxy group in the 6-position of the GlcNAc residues is not involved in protein binding and is sterically suited for the attachment of a spin label. Therefore, we replaced this hydroxy group of one or both GlcNAc moieties of **1–3** with an amine and attached a nitroxide label through an amide bond (Scheme 1; for details of the synthesis see the Supporting Information).

All EPR experiments were carried out at a ligand concentration of 33 μM . For DEER experiments, samples were annealed either in the presence or absence of WGA in aqueous solutions containing 30% (v/v) glycerol. The measurements were performed at a temperature of 40 K after shock-freezing in liquid nitrogen in order to trap the annealed conformation (for details and baseline-subtracted DEER data see the Supporting Information). Distance distributions were obtained by a model-free analysis using DEERAnalysis 2009.^[11]

DEER experiments performed with a solution of divalent doubly spin-labeled ligand **1₂** in the absence of WGA revealed a broad distance distribution with significant contributions below 2 nm (Figure 1, bottom) and even below 1.5 nm as

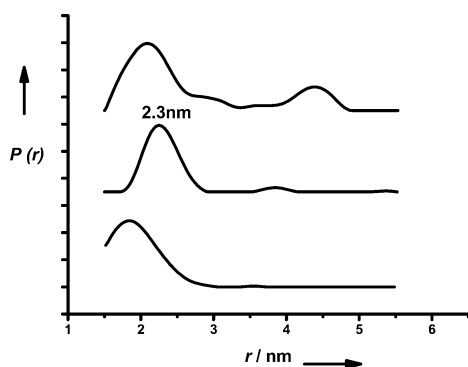


Figure 1. Distance distributions from DEER analysis for doubly spin-labeled divalent ligand **1₂** in the absence (bottom) and presence of WGA (molar ratio WGA dimer/ligand **1₂** 8:1 (center) and 1:4 (top)). The peak at 2.3 nm (center) is attributed to the bridging of adjacent primary binding sites; additional distances (top) correspond to inter-ligand distances between ligands bound to the same WGA dimer.

detected by cw EPR (Supporting Information, Figure S1). This can be explained by the flexibility of the linker between the two spin-labeled GlcNAc moieties which allows the sampling of many conformations with varying distances between the spin labels (Figure 2 a). The rotational diffusion of the spin label attached to **1₁** at room temperature is fast ($\tau_c = 120$ ps, Figure S2, bottom) as expected for a molecule of this size.

Upon addition of an eightfold molar excess of the WGA dimer, we expect almost quantitative binding of **1** to the protein, assuming the IC_{50} value of the ligand is similar to its K_D . Accordingly, the rotational mobility of the singly labeled ligand **1₁** was found to be significantly decreased under these

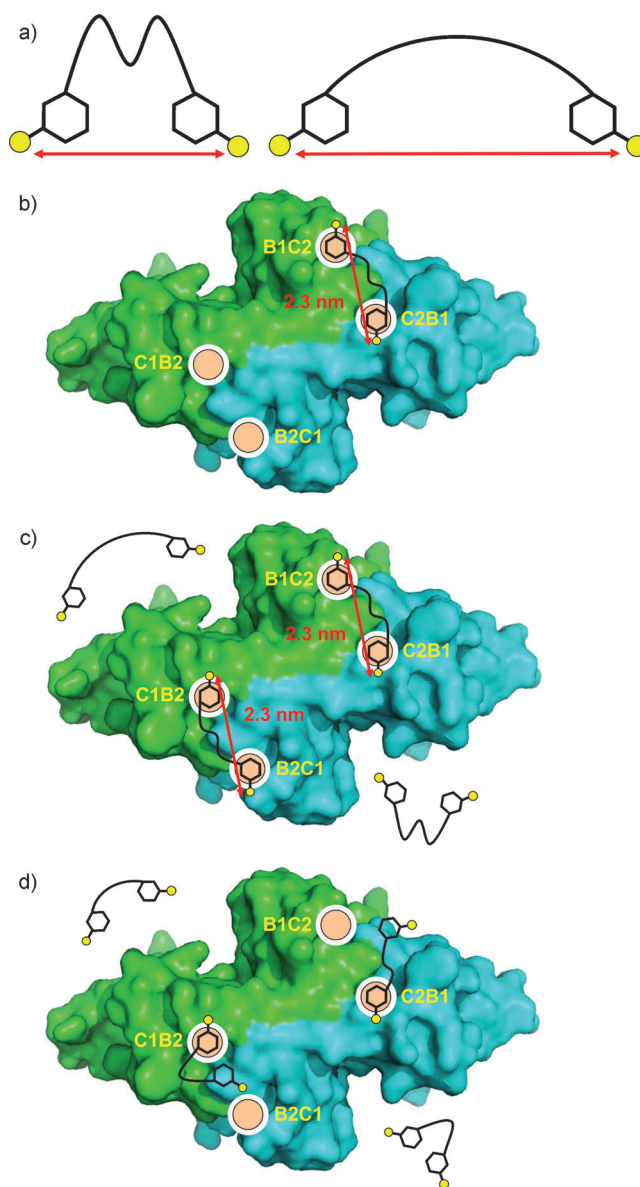


Figure 2. a) Divalent ligand **1₂** in solution; the flexible linker allows the sampling of many conformations which have varying distances between the spin labels. Proposed binding mode of **1₂** in the presence of b) an excess of WGA dimer and c) an excess of ligand **1₂**. d) Proposed binding mode of divalent **1₂** in the presence of an excess of WGA dimer. The two subunits of the WGA dimer are colored blue and green. Nitroxide spin labels are depicted as yellow circles.

conditions ($\tau_c = 1.8$ ns, Figure S2, center) confirming quantitative binding. Also, the distribution of distances between the two spin labels within **1₂** has changed significantly. The width of the distance distribution has become narrower and its peak maximum has shifted to 2.3 nm; no distances below 1.5 nm are evident (Figure 1, center; Figure S1, center). This correlates well with a stretched divalent ligand binding simultaneously with both sugars to the protein (Figure 2 b). Given the 8:1 protein/ligand molar ratio, statistically not more than one divalent ligand is bound to one WGA dimer. Quantitative analysis of the distance distribution taking into account the conformation of the bound ligand according to the crystal

structure (PDB entry 2X52) as well as the dimensions and orientational flexibility of the spin labels (Figures S4 and S5), reveals that the ligand bridges pairs of adjacent primary binding sites (B1C2/C2B1 or B2C1/C1B2).

If we decrease the lectin concentration to a WGA dimer/ligand molar ratio of 1:4, only a fraction (<40%) of the divalent ligand is expected to bind to WGA. Mobility measurements (Figure S2, top) also suggest only partial binding. Partial binding is also reflected in the distance distribution between the two spin labels within **1**₂ (Figure 1, top) with the low-distance peak featuring a broader shoulder at the lower distance end and a shift of its maximum to a slightly smaller distance. This suggests a superposition of the distance distributions for bound and for unbound ligands, respectively. Corresponding simulations suggest about 40% bound ligands. In addition, the measurements of the shorter distances using cw spectra at low temperatures (Figure S1, top) indicate a reduced—compared to in the absence of WGA (Figure S1, bottom)—but still significant presence of short distances ($r < 1.5$ nm) allocated to unbound ligands. While the relative binding fraction of the divalent ligand is decreased at the reduced protein concentration, the number of bound ligands per protein is increased, that is, larger than 1 (Figure 2c). Consequently, additional distances appear in the distribution (Figure 1, top) corresponding to interligand spin interactions between different molecules of **1**₂ bound to the very same WGA dimer. While a quantitative analysis for multiple spin interactions is difficult,^[12] a prominent peak at $r = 4.3$ nm and a broad feature for $r < 4$ nm can be identified. These distances correspond very well to the interligand distances between the primary binding sites predicted from the crystal structure (cf. Figure S4, distances between oxygens in the 6-position of GlcNAc residues: 4.2, 2.6, and 3.5 nm). The interligand distances between the secondary binding sites D2A1 and D1A2 (up to 5.3 nm) are not found.

For the divalent ligands **2**₁ and **2**₂ with the short linker we find in the absence of WGA a situation similar to that for **1**₁ and **1**₂, respectively. Rotational diffusion of **2**₁ is fast ($\tau_c = 120$ ps, Figure S6, bottom), distances shorter than 1.5 nm are present (Figure S7, top), and the distance distribution obtained from DEER analysis of **2**₂ features a single broad peak with a maximum at 1.8 nm (Figure 3, bottom). This maximum occurs at the same distance as for **1**₂. This can be explained by the *gauche* effect of the oxygen atoms in the linker region of **1**₂ leading to a folded conformation that is well known for oligo(ethylene glycol) chains.^[13] Upon addition of WGA, the results for the shorter ligand **2**₂ completely from those obtained with **1**₂. Even in the presence of an eightfold molar excess of the WGA dimer, the main component of the cw spectrum of **2**₁ at room temperature remains the fast motion regime as in the absence of WGA. Only a small fraction features a reduced mobility (Figure S6, top). This finding suggests a low binding affinity which is in accordance with the IC_{50} value of **2**. In the distance distribution obtained with **2**₂ under these conditions (Figure 3, top), the same short distances as those in absence of WGA are found (including distances below 1.5 nm; cf. Figure S7). Distances of $r = 2.3$ nm corresponding to the stretched, site-bridging ligand conformation do not appear

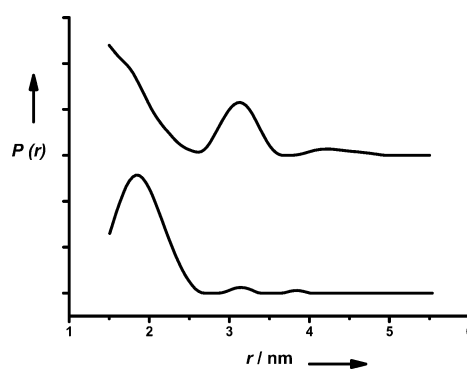


Figure 3. Distance distributions for **2**₂ in the absence (bottom) and presence of WGA (molar ratio WGA dimer/ligand **2**₂ 8:1, top). Small peaks at $r = 3.1$ and 3.9 nm (bottom) are not significant (see the Supporting Information).

significantly. In contrast, distances around 3 nm are present that are attributed to interligand distances between spin-labeled ligands bound to C1B2 and C2B1. From these findings we conclude that there is a small fraction of monovalently bound divalent ligands which preferably bind to C1B2 and C2B1 (Figure 2d). The absence of the typical prominent peak at $r = 2.3$ nm observed for **1**₂ shows that under these conditions adjacent binding sites, for example C1B2 and B2C1, are not occupied simultaneously. Since the crystal structure does not suggest steric hindrance of simultaneous binding to adjacent binding sites, the most plausible explanation for this observation is that the binding affinity for C1B2 and C2B1 is higher than for the other two primary binding sites.

In a solution of monovalent ligand **3**₁ and WGA (each $33 \mu\text{M}$), only weak binding is detected by EPR spectroscopy. The main contribution to the dipolar evolution in the DEER experiment originates from the background signal of a homogeneous three-dimensional spin distribution. However, there is a small contribution from interacting spins of singly labeled ligands **3**₁ bound to the very same WGA dimer. The peak at 2.3 nm which is characteristic for binding to adjacent binding sites is missing (Figure 4, bottom) as in the case of **2**₂. Only longer distances allocated to distances between the binding sites C1B2 and C2B1 (around 3 nm, cf. Figure 3, top) and between B1C2 and B2C1 (around 4 nm) occur. Not until the WGA concentration is decreased to a protein/ligand molar ratio of 1:7, resulting in more ligands bound per protein, does the peak attributed to adjacent binding sites appear (Figure 4, top). The increase of the relative intensity of the peak allocated to the occupied binding sites B1C2 and B2C1 (approximately 4 nm) with decreasing protein/ligand ratio, again, indicates the lower binding affinity of these sites compared to C1B2 and C2B1.

In summary, our results show a detailed picture of the molecular mechanism of the binding of mono- and divalent ligands to WGA. Applying a combination of state-of-the-art EPR techniques, we obtained, for the first time, structural evidence for multivalent protein–ligand interactions in solution. The chelating binding of the divalent ligand **1**₂, which has a linker long enough to bridge adjacent binding sites, is

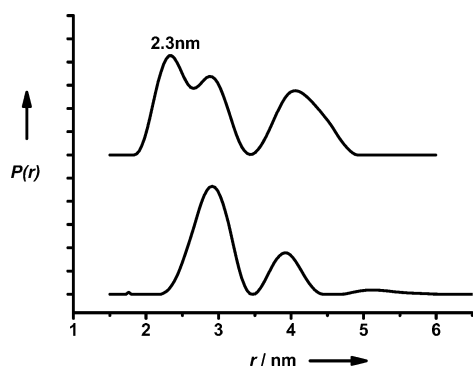


Figure 4. Distance distributions for 3_1 in the presence of WGA (molar ratio WGA dimer/ligand 3_1 1:1 (bottom) and 1:7 (top)).

directly detected and can be differentiated from the monovalent binding of multiple molecules of the divalent ligand 2_2 , which has a linker that is too short to bridge binding sites. In addition, analysis of intermolecular spin interactions between different ligand molecules of 2_2 or 3_1 bound to the same multivalent protein molecule provides hints as to which binding sites are preferentially occupied. The technique presented here is not confined to WGA but has broad applicability to the analysis of many multivalent protein–ligand interactions.

Received: February 12, 2011
 Published online: July 7, 2011

Keywords: carbohydrates · EPR spectroscopy · ligands · multivalency · proteins

- [1] a) Y. C. Lee, R. T. Lee, *Acc. Chem. Res.* **1995**, *28*, 321–327; b) M. Mammen, S.-K. Choi, G. M. Whitesides, *Angew. Chem.* **1998**, *110*, 2908–2953; *Angew. Chem. Int. Ed.* **1998**, *37*, 2754–2794; c) J. J. Lundquist, E. J. Toone, *Chem. Rev.* **2002**, *102*, 555–578; d) B. E. Collins, J. C. Paulson, *Curr. Opin. Chem. Biol.* **2004**, *8*, 617–625; e) V. Wittmann, S. Seeberger, *Angew. Chem.* **2004**, *116*, 918–921; *Angew. Chem. Int. Ed.* **2004**, *43*, 900–903; f) L. L. Kiessling, J. E. Gestwicki, L. E. Strong, *Angew. Chem.* **2006**, *118*,

- 2408–2429; *Angew. Chem. Int. Ed.* **2006**, *45*, 2348–2368; g) A. Imberty, A. Varrot, *Curr. Opin. Struct. Biol.* **2008**, *18*, 567–576.
- [2] a) T. K. Dam, C. F. Brewer, *Biochemistry* **2008**, *47*, 8470–8476; b) R. J. Pieters, *Org. Biomol. Chem.* **2009**, *7*, 2013–2025.
- [3] a) P. I. Kitov, J. M. Sadowska, G. Mulvery, G. D. Armstrong, H. Ling, N. S. Pannu, R. J. Read, D. R. Bundle, *Nature* **2000**, *403*, 669–672; b) E. A. Merritt, Z. Zhang, J. C. Pickens, M. Ahn, W. G. J. Hol, E. Fan, *J. Am. Chem. Soc.* **2002**, *124*, 8818–8824; c) Z. Zhang, E. A. Merritt, M. Ahn, C. Roach, Z. Hou, C. L. M. J. Verlinde, W. G. J. Hol, E. Fan, *J. Am. Chem. Soc.* **2002**, *124*, 12991–12998.
- [4] D. Schwefel, C. Maierhofer, J. G. Beck, S. Seeberger, K. Diederichs, H. M. Möller, W. Welte, V. Wittmann, *J. Am. Chem. Soc.* **2010**, *132*, 8704–8719.
- [5] a) H. Kessler, G. Zimmermann, H. Foerster, J. Engel, G. Oepen, W. S. Sheldrick, *Angew. Chem.* **1981**, *93*, 1085–1086; *Angew. Chem. Int. Ed. Engl.* **1981**, *20*, 1053–1055; b) M. J. N. Junk, H. W. Spiess, D. Hinderberger, *Angew. Chem.* **2010**, *122*, 8937–8941; *Angew. Chem. Int. Ed.* **2010**, *49*, 8755–8759; c) J. F. Espinosa, J. L. Asensio, J. L. Garcia, J. Laynez, M. Bruix, C. Wright, H.-C. Siebert, H.-J. Gabius, F. J. Canada, J. Jimenez-Barbero, *Eur. J. Biochem.* **2000**, *267*, 3965–3978.
- [6] a) C. S. Wright, *J. Mol. Biol.* **1980**, *141*, 267–291; b) C. S. Wright, *J. Mol. Biol.* **1989**, *209*, 475–487; c) K. Harata, H. Nagahora, Y. Jigami, *Acta Crystallogr. Sect. D* **1995**, *51*, 1013–1019.
- [7] C. S. Wright, G. E. Kellogg, *Protein Sci.* **1996**, *5*, 1466–1476.
- [8] C. Maierhofer, K. Rohmer, V. Wittmann, *Bioorg. Med. Chem.* **2007**, *15*, 7661–7676.
- [9] a) A. Milov, K. Salikhov, M. Shirov, *Fiz. Tverd. Tela* **1981**, *23*, 975–982; b) A. D. Milov, A. B. Ponomarev, Y. D. Tsvetkov, *Chem. Phys. Lett.* **1984**, *110*, 67–72; c) M. Pannier, S. Veit, A. Godt, G. Jeschke, H. W. Spiess, *J. Magn. Reson.* **2000**, *142*, 331–340; d) A. K. Upadhyay, P. P. Borbat, J. Wang, J. H. Freed, D. E. Edmondson, *Biochemistry* **2008**, *47*, 1554–1566; e) J. Bhatnagar, P. P. Borbat, A. M. Pollard, A. M. Bilwes, J. H. Freed, B. R. Crane, *Biochemistry* **2010**, *49*, 3824–3841; f) P. P. Borbat, J. H. Freed, *Methods Enzymol.* **2007**, *423*, 52–116.
- [10] A. Milov, B. Naumov, Y. Tsvetkov, *Appl. Magn. Reson.* **2004**, *26*, 587–599.
- [11] G. Jeschke, A. Koch, U. Jonas, A. Godt, *J. Magn. Reson.* **2002**, *155*, 72–82.
- [12] G. Jeschke, M. Sajid, M. Schulte, A. Godt, *Phys. Chem. Chem. Phys.* **2009**, *11*, 6580–6591.
- [13] *Poly(Ethylene Glycol) Chemistry. Biotechnical and Biomedical Applications* (Ed.: J. M. Harris), Plenum, New York, **1992**.